Li, W-C., Soffe, S. R., & Roberts, A. (2003). The spinal interneurons and properties of glutamatergic synapses in a primitive vertebrate cutaneous flexion reflex. Journal of Neuroscience, 23(27), 9068 - 9077.

lietal703.doc Behavioral/Systems Neuroscience

The spinal interneurons and properties of glutamatergic synapses in a primitive vertebrate cutaneous flexion reflex.

By W.-C. Li, S. R. Soffe, and Alan Roberts

School of Biological Sciences, University of Bristol, Woodland Road, Bristol, BS8 1UG, U.K.

Abbreviated Title: Spinal interneuron connectivity.

Number of text pages:
Number of figures: 9
Number of tables: 0

Number of words in Abstract: 249
Number of words in Introduction: 500
Number of words in Discussion: 1499

Author for correspondence:
Dr Wen-Chang Li, School of Biological Sciences, University of Bristol, Woodland Road, Bristol, BS8 1UG, United Kingdom.
Phone: (+44) 117 9287 488
FAX: (+44) 117 9257 374
E-mail: wenchang.li@bristol.ac.uk

Acknowledgements: We should like to thank Tim Colborn, Derek Dunn and Bob Porter for technical assistance and the Wellcome Trust for support.

Key words: Locomotion, reflex, spinal cord, NMDA, glutamate receptors, *Xenopus*.

ABSTRACT
Unlike the monosynaptic “stretch” reflex, the exact neuronal pathway for a simple cutaneous reflex has not yet been defined in any vertebrate. In young frog tadpoles we have made whole-cell recordings from pairs of spinal neurons. We have found direct, excitatory, glutamatergic synapses from touch sensitive skin sensory neurons to sensory pathway interneurons, and then from these sensory interneurons to motoneurons and premotor interneurons on the other side of the body. We conclude that the minimal pathway for this primitive reflex, where stroking the skin on one side leads to flexion on the other side, is disynaptic. This detailed circuit information has allowed us to ask whether the properties of glutamatergic synapses during the first day of CNS development are tuned to their function in the tadpole’s responses. Stroking the skin excites a few sensory neurons. These activate mainly AMPA receptors producing short, strong excitation that activates many sensory pathway interneurons but only allows temporal summation of closely synchronous inputs. In contrast, the excitation produced in contralateral neurons by the sensory pathway interneurons is weak and mainly mediated by NMDA receptors. As a result, considerable summation is required for this excitation to lead to post-synaptic neuron firing and a contralateral flexion. We conclude that from their early functioning, synapses from sensory neurons are strong and from sensory pathway interneurons are weak. The distribution of glutamate receptors at synapses in this developing circuit is tuned so that synapses have properties suited to their roles in the whole animal’s reflex responses.

INTRODUCTION
This study addresses one main question. How is the primitive vertebrate spinal flexion reflex organised? Though most textbooks of neuroscience show the mammal flexion reflex with two layers of interneurons in the pathway, we know of no case in the vertebrates where the spinal pathway from a skin stimulus to a motor response can be traced, synapse by synapse, from the sensory receptors, via defined interneurons to the motoneurons. It also sheds some light on a second question, what happens when central glutamatergic synapses develop in such a pathway? Do they start as “silent” synapses with just NMDA receptors (NMDARs), only later acquiring AMPA receptors (AMPARs) and becoming functional as a result of activity (Feldman and Knudsen, 1998; Zhu and Malinow, 2002), or, are synapse properties activity independent and tuned to their circuit functions from an early stage (Renger et al., 2001; Ziv and Garner, 2001)? We examine these questions by exploiting the frog tadpole spinal cord where there are few interneuron types (Roberts et al., 2000; Li et al., 2001) and whole-cell recordings can be made from pairs of neurons to look at synaptic interactions (Li et al., 2002).

In hatchling *Xenopus* tadpoles, stroking the skin on one side of the trunk can lead to a flexion on the opposite side followed by swimming away (Boothby and Roberts, 1995). Can we trace the cellular components of this response pathway? The trunk skin is innervated by one class of sensory neuron in the dorsal spinal cord called *Rohon-Beard* (RB) neurons. These respond to touch and strokes, adapt very rapidly and can also be excited by current pulses to the skin (Clarke et al., 1984). In the dorso-lateral spinal cord there are sensory pathway *dorsolateral commissural* interneurons (dlc) with dendrites in positions to contact the longitudinal central axons of *Rohon-Beard* neurons. These dlc interneurons have axons that project to the opposite side of the cord. Intracellular recordings with dye injection have shown that they are excited at short latency following touch or current pulses to the skin, so they are presumed to be excited directly by the axons of the sensory RB neurons (Clarke et al., 1984; Roberts and Sillar, 1990). Recordings from unidentified spinal interneurons have shown that RB neurons release a transmitter, presumed to be glutamate, that activates NMDARs and non-NMDARs to produce

strong excitation (Sillar and Roberts, 1988a). Following skin stimulation, unidentified ventral neurons on the opposite side of the spinal cord, that are rhythmically active during swimming, receive excitation. Indirect evidence supports the proposal that this excitation comes from dlc interneurons, is glutamate mediated, and activates NMDARs (Roberts and Sillar, 1990).

Our aim was to use paired recordings with dye injection to confirm the identity of the sensory pathway interneurons excited by sensory RB neurons and to find which neurons the sensory pathway interneurons themselves excited on the opposite side. Using this detailed circuit information, we asked whether the properties of glutamatergic synapses between these neurons are homogeneous at this early stage of CNS development, or are tuned to their functions in this simple reflex pathway.

METHODS

Details of the methods have been given recently (Li et al., 2002). Briefly, *Xenopus* tadpoles at stage 37/38 (see Fig. 2A) were anaesthetised with 0.1% MS-222 (3-aminobenzoic acid ester, Sigma, UK), then pinned in a small bath of saline (concentrations in mM: NaCl 115, KCl 3, $CaCl_2$ 2, $NaHCO_3$ 2.4, $MgCl_2$ 1, HEPES 10, adjusted with 5M NaOH to pH 7.4). In many paired recording experiments, 1mM $MgCl_2$ was replaced by 1mM $CaCl_2$. The dorsal fin was cut and the tadpole transferred to 10 μM α-bungarotoxin saline. After immobilization, the tadpole was re-pinned so that skin and muscles over the right side of the spinal cord could be removed. A dorsal cut was then made along the midline of the spinal cord to open the neurocoel and expose neuronal cell bodies. Further small cuts were made to expose more ventral neurons. In experiments on transmission from dlc interneurons to contralateral rhythmic neurons, the right side of the spinal cord in segments 3 to 5 was removed to allow better illumination in order to see and access left side neurons better. The animal was then re-pinned on a small rotatable Sylgard stage in a 700 μl recording chamber that allowed brightfield illumination from below on an upright Nikon E600FN microscope. The animal was tilted to an angle which allowed the exposed neuronal cell bodies on the left and right sides of the cord to be seen using a x40 water immersion lens. Saline in the chamber was circulated at about 2 ml per minute. Drops of antagonists were added to a 100 μl chamber upstream to the recording chamber (bath application) or applied close to the recorded neuron soma by applying gentle pressure to solution in a pipette with tip diameter of 20-30 μm (microperfusion). Unless specified, the concentrations for 1,2,3,4-tetrahydro-6-nitro-2,3-dioxo-benzo[f]quinoxaline-7-sulfonamide (NBQX), D-2-amino-5-phosphonopentanoic acid (D-AP5) and Mg^{2+} used in this paper were 5μM, 50 μM and 1 mM, respectively. NBQX and D-AP5 were obtained from Tocris (UK); mecamylamine and strychnine were from Sigma (UK).

Extracellular recordings of ventral root activity were made using glass suction electrodes placed against the intermyotome clefts. A stimulating suction electrode was placed on the head or tail skin to start fictive swimming activity. Patch pipettes were filled with 0.1% neurobiotin in intracellular solution (concentrations in mM: K-gluconate 100mM, $MgCl_2$ 2mM, EGTA 10mM, HEPES 10mM, Na_2ATP 3mM, NaGTP 0.5 mM adjusted to pH 7.3 with KOH) and had resistances around 10 MΩ. Patch pipettes were advanced under visual control to contact exposed neuron somata. Positive pressure (5-20 cm H_2O) was always applied to the pipette solution before trying to get a seal. Signals were recorded with an Axoclamp 2B in conventional bridge or continuous single electrode voltage clamp mode. Data were acquired with Signal software through a CED 1401 Plus with sampling rate of 10 kHz. Stimuli to the skin were controlled using the CED 1401 Plus configured by Signal and given via an optically coupled isolator. Offline analyses were made with Minitab and Excel. All data were tested for normality

(Anderson-Darling); median values are given for non-normal data, otherwise all values are given as mean ± S.D.

In patch pipette recordings from pairs of neurons, current induced spikes in one cell caused a small cross-talk artefact in the other (Li et al., 2002). These artefacts were sometimes removed from recordings where they obscured the onset of small EPSPs evoked by current induced spikes. To do this, averaged records of EPSP failures (artefact alone) were subtracted from EPSP records (EPSP plus artefact).

Once physiological testing was completed, trains of positive current pulses (10-100 pA, 500 msec duration) were applied for 2-5 minutes to label recorded neurons with neurobiotin. The tadpoles were then left for 30 minutes before fixing in 2% glutaraldehyde in 0.1 M phosphate buffer (pH 7.2 at ~4°C). After rinsing with 0.1 M phosphate buffered saline (120 mM NaCl in 0.1 M phosphate buffer, pH 7.2; PBS), the animals were: (1) washed in 1% triton-X in PBS for 15 minutes twice; (2) incubated in a 1:300 dilution of extravidin peroxidase conjugate (Sigma) in PBS containing 0.5% Triton-X for 2-3 hours; (3) washed again in PBS; (4) pre-soaked in 0.08% diaminobenzidine in PBS (DAB solution) for 5 minutes; (5) moved to 0.075% hydrogen peroxide in DAB solution for 5 minutes; (6) washed in running tap water. The brain and spinal cord were then dissected free with the notochord and some ventral muscles, dehydrated, cleared in methyl benzoate and xylene, and mounted whole, between two coverslips using Depex.

Neurons were observed using a x100 oil immersion lens and traced using a drawing tube. To compensate for shrinkage during dehydration, all measurements in this paper have been corrected by multiplying by 1.28 (Li et al., 2001).

RESULTS

Short latency flexion reflex to tail skin stimulation

By making recordings from the motor nerves (ventral roots) in the mid-trunk swimming muscles on both sides of the tadpole's body, we have defined the normal response of spinal motoneurons to tail skin stimulation. To allow us to measure latencies accurately we used a 1 ms current pulse to excite the peripheral neurites of primary touch sensitive Rohon-Beard (RB) neurons that innervate the skin (Clarke et al., 1984). Typically, the first motoneuron activity is a brief, short-latency ventral root burst on the opposite side (Fig. 1A). This is then followed by the onset of swimming. The latency of the initial contralateral response to a near-threshold stimulus was measured for 8 animals and lay in the range 7.0-13.8 msec (11.5 ± 2.7 msec).

Connections from skin sensory neurons to sensory pathway interneurons

In *Xenopus* tadpoles we have detailed anatomical definitions for spinal sensory neurons, motoneurons and interneuron classes (Clarke and Roberts, 1984; Roberts et al., 1999; Li et al., 2001). We also know about the responses of most of these neurons to skin stimulation, their activity during fictive swimming and details about some of their synaptic connections (Dale, 1985; Dale and Roberts, 1985; Li et al., 2002). We therefore knew the candidate neurons in the pathway from touching the skin on one side to activity in motoneurons on the other (Fig. 1B). We first examined connections from sensory neurons (RB) to sensory interneurons (dlc interneuron) in the dorsolateral region of the cord.

With the spinal cord opened along its dorsal midline, RB neurons can be recognized by their large size and position at the cut surface. We made simultaneous recordings from RB neurons and 48 other neurons with somata exposed by the dorsal cut, using a 0 Mg^{2+} saline so the NMDAR mediated component of glutamatergic excitation would be clear. Possible RB neurons showed no response or a single spike to skin stimulation, and no input during fictive swimming

(Clarke et al., 1984). Possible dlc interneurons showed a short-latency EPSP to skin stimulation that often led to an action potential, and were inhibited during fictive swimming (Clarke and Roberts, 1984; Roberts and Sillar, 1990). In 28 of these paired recordings, intracellular current injection that evoked an action potential in the RB neuron led to a large EPSP in the other neuron (Fig. 2). In 15 cases the EPSP was sufficient to evoke an action potential from the resting membrane potential. Later anatomical processing confirmed the identification of RB neurons by their spherical soma, absence of dendrites and ascending and descending central axons in the dorsal spinal cord (Clarke et al., 1984). The anatomy also showed that each post-synaptic neuron had the features of dlc interneurons: a dorsolateral, multipolar soma with a number of dendrites, and a ventral initial process leading to a ventral commissural axon that projects towards the brain where it branches to project at least a short distance towards the tail on the opposite side (Fig. 2A; Roberts and Sillar, 1990; Li et al., 2001).

EPSPs were examined for 15 neuron pairs in which the anatomy of pre-synaptic RB neuron and post-synaptic dlc interneuron were clear. Median EPSP amplitude for each pair ranged from 3.4-25.4 mV and maximum amplitudes ranged from 6.5-33.5 mV. EPSP amplitude did not correlate with the dlc interneuron resting potential (–61.7±5.8 mV). All EPSPs had a fast rise in the range from 1.1 to 2.9 msec (overall median 1.6 msec). For 14 pairs, EPSP duration at 50% peak amplitude ranged from 5.5-22.9 msec (12.6±5.9 mV). For one pair, the duration was much longer (median 132.3 msec) suggestive of a polysynaptic component. The fast rise and relatively short duration suggested that the other EPSPs were mainly produced by activation of non-NMDARs.

If RB axons make direct monosynaptic connections onto dlc interneurons then EPSP latencies should be short and consistent. All EPSP latencies were short, in the range 1.4-3.4 msec (2.34±0.55 msec, n = 15 neuron pairs; measured from the peak of the pre-synaptic spike to 10% of the peak amplitude on the EPSP). Consistent latency was shown by a low standard deviation in latency values for each pair (range 0.05-0.51 msec). The distances between the RB and dlc interneuron somata were 0.09-0.61 mm when measured anatomically from the neurobiotin fills. For each pair, the minimum EPSP latency increased significantly with conduction distance (p = 0.027). Assuming a conduction velocity for the RB axons of 0.3 m/sec (the modal value quoted by Clarke *et al*., 1984), we estimated the mean synaptic delay to be ~1.0 msec. This is fully compatible with the connection between RB axons and dlc interneurons being monosynaptic.

To investigate the receptors activated when RB action potentials led to excitation of dlc interneurons, we looked at the effects of the specific NMDAR antagonist D-AP5 and AMPAR antagonist NBQX, and of 1mM Mg^{2+}, which would be expected to block any voltage dependent NMDAR mediated component. When the antagonists were applied during paired recordings, EPSPs evoked in dlc interneurons by RB impulses appeared to be completely blocked by 5μM NBQX (n=12) but were little affected by AP5 (n=8, Fig. 3) or 1mM Mg^{2+} (n=4, data not shown).

To determine whether excitation of anatomically identified dlc interneurons was mainly AMPAR mediated, as suggested by the short time course, we recorded dlc interneuron responses to electrical stimulation of RB processes in the ipsilateral tail skin (Fig. 4). Under both current-clamp (n=10) and voltage-clamp (n=9), these recordings showed that the fast early component of excitation, blocked by NBQX, provided the majority of the peak potential or current (see below). The slower, longer component, blocked by AP5 and 1mM Mg^{2+} was much smaller. The AMPAR and NMDAR currents were separated pharmacologically by addition of D-AP5 or NBQX respectively (Fig. 4C). The peak current was then measured under voltage clamp (at –65 mV) for nine dlc interneurons. Peak AMPAR current was ~2 msec after EPSC onset and ranged from

101-444 pA. Peak NMDAR current was at ~20-30 msec after EPSC onset and ranged from 3-36 pA. Based on these peak currents, the AMPAR/NMDAR ratio for the nine neurons was 28.0±31.7 (range 6.5-108.0). The synapses from RB to dlc interneurons are therefore dominated by AMPAR mediated excitation.

We conclude from these results that sensory RB neurons synapse directly with sensory pathway dlc interneurons, and release glutamate that activates mainly AMPAR to produce strong excitation where individual EPSPs can often lead to dlc interneuron action potentials.

Connections from dlc interneuron to contralateral neurons

To investigate the synaptic connections from dlc interneurons we made 58 simultaneous recordings from dlc interneurons on the right side of the spinal cord and neurons on the contralateral, left side. In many cases the medial surfaces of the somata of neurons on the left side were exposed in more ventral regions by making small cuts in the wall of the central canal. All these neurons were identified by examining their anatomical features after the experiment. They all showed rhythmic activity during fictive swimming (not illustrated) and their responses to right side (contralateral) skin stimulation were recorded.

Ten of the left side neurons were identified as motoneurons (mn, Fig.5A). Since muscles had to be removed at an early stage in the dissection, peripheral axons that would give unambiguous identification of motoneurons were often lost. In these cases we therefore adopted the following criteria for identification (based on Roberts et al., 1999): a multipolar soma, a short ventral descending axon (<100 μm in length), a possible broken axon end at the surface of the spinal cord, no broken axon end near ventral midline. When current evoked an action potential in the right side dlc interneuron, 6 motoneurons received small, long duration, short-latency EPSPs (Fig. 5BC).

The remaining 45 left side neurons were premotor interneurons belonging to three anatomical classes. *Commissural interneurons* (cINs; *n* = 36) are glycinergic and produce reciprocal inhibition during both swimming and struggling (Dale, 1985; Soffe, 1993). These cINs have unipolar somata, an initial ventral process with short dendrites and a ventral commissural axon that branches to ascend and descend contralaterally (Fig. 5D; Yoshida et al., 1998). In 18 cases, dlc interneurons produced small, long duration, short-latency EPSPs in cINs (Fig. 5EF).

Six *ascending interneurons* (aINs) were recorded with dlc interneurons and in four cases there were synaptic connections. These glycinergic interneurons have unipolar somata lying in the dorsal half of the cord with mainly ventral dendrites (Fig. 6A). They have an ascending axon that branches near the soma to give a descending axon. They are active during swimming and produce gating inhibition of sensory pathway dlc interneurons (Li et al., 2002). Impulses in dlc interneurons led to small, long duration, short latency EPSPs in all 4 aINs.

Three examples of *descending interneurons* (dINs) were recorded with dlc interneurons. These are thought to be the excitatory, glutamatergic interneurons responsible for excitatory drive during swimming (Dale and Roberts, 1985). They have multipolar somata and a descending ipsilateral axon (Li et al., 2001; Fig. 7A). In 1 paired recording dlc interneuron impulses led to a small EPSP in a dIN (not illustrated).

The EPSPs evoked by dlc interneuron impulses in contralateral neurons (motoneurons and interneurons) differed from RB-evoked EPSPs in dlc interneurons in three ways. Firstly, they had significantly lower peak amplitudes (combined measurements from 22 neurons: 2.9 ± 2.5 mV;

range 0.6-11.8 mV; Mann-Whitney: $p<0.001$). Secondly, the rise times of EPSPs varied widely but were of broadly two types. Some (~70%) were relatively slow, ranging from 10-40 msec (n =15; Figs. 5E, 6B); the remainder (~30%) were clearly fast(<5 msec; n = 6; Figs. 5B, 6C). Thirdly, the EPSPs had a significantly longer duration (combined measurements from 20 neurons at half peak amplitude: 68.4 $\pm$ 49.4 msec; range 14–236 msec; Mann-Whitney: $p<0.001$; Fig. 5CF).

In some of these motoneuron and premotor IN recordings, the small size and short latency of the EPSP meant that its onset could not be clearly distinguished from the coupling artefact produced by the presynaptic impulse (eg Figs 5E, 6B). However, the onset was clear in averaged records from the remaining 18 examples, following subtraction of the artefact (see Methods, Fig 5A, 6C). Latencies in these examples (with distances between pre- and post-synaptic neuron from 0.2-0.7 mm) ranged from 0.8 to 3.1 msec and the mean value with its low SD (1.72 $\pm$ 0.62 msec) was similar to that for RB to dlc interneuron synapses. Assuming the same conduction velocity for the dlc axons as used for RB axons above (0.3 m/sec; Clarke *et al*., 1984), we estimated the mean synaptic delay to be ~0.2 msec. This rather low value suggests that the conduction velocity for dlc axons may actually be faster than for RB axons, but is still fully compatible with dlc interneurons making direct, monosynaptic connections to contralateral neurons.

We conclude that motoneurons and the three known premotor interneuron classes that are active during swimming (a*INs, dINs* and *cINs)* all receive direct weak excitation from contralateral dlc interneurons.

Pharmacological properties of synapses in contralateral neurons

The long duration of EPSPs evoked in contralateral neurons by dlc interneuron impulses, together with the long rise-time of some EPSPs suggested the presence of a significant NMDAR mediated component. Application of D-AP5 and NBQX to EPSPs evoked by spikes in a single dlc interneuron (n = 7 neuron pairs; Fig. 6BE) or by a current pulse to the contralateral tail skin (n = 8 neurons; not illustrated) showed that most of these EPSPs had both an AMPAR and NMDAR component (Fig. 6). The NMDAR component of the EPSP was relatively larger than for EPSPs in dlc interneurons. Similar results were obtained for nine additional neurons under voltage clamp (1 motoneuron, 8 interneurons) in which EPSCs were evoked by a current pulse to the contralateral tail skin (Figs 7C, 8A-C). The long NMDAR component of the dlc interneuron evoked EPSC was also blocked by adding 1mM Mg^{2+} to the bathing saline (n = 6; Fig. 8D).

In contrast to the strong AMPAR component that dominated the excitation in dlc interneurons, the AMPAR component of dlc interneuron output synapses was very variable. In some paired records the AMPAR component appeared to be absent (Fig 6Bb) but in others it was larger. Under voltage clamp, some EPSCs had a significant AMPAR component and showed a fast rise (<5 msec to peak, e.g. Fig. 5C, 6C), while others had little or no AMPAR component and showed a much slower rise (~20 msec or more to peak; Fig. 5F, 6B, 7B).

The relative contributions of AMPAR and NMDAR currents were measured under voltage clamp for EPSCs evoked by stimulation of the contralateral tail skin in nine neurons (1 motoneuron and 8 interneurons, Figs. 7C, 8B-D). As for EPSCs in dlc interneurons, the peak AMPAR current was ~2 msec after EPSC onset but was smaller and ranged from only 2-108 pA. Peak NMDAR current was ~20-30 msec after EPSC onset and ranged from 6-84 pA. The AMPAR/NMDAR ratio based on these peak currents was 1.51 $\pm$ 1.43 (range 0.23-4.64). A very similar ratio of 1.31 $\pm$ 0.62 (range 0.30-2.05) was obtained in 6 additional motoneurons by comparing the amplitudes of EPSCs at 2 msec and 20 msec from the onset, which is equivalent to the times of

peak AMPAR and peak NMDAR currents revealed pharmacologically. The AMPAR/NMDAR ratio for motoneuron and IN EPSCs was significantly lower than the ratio of 28.0 $\pm$ 31.7 for EPSCs in dlc interneurons (Mann-Whitney: p<0.001). Unlike the EPSCs evoked by RBs in dlc interneurons, therefore, the EPSCs that dlc interneurons evoke in neurons on the opposite side of the spinal cord have a significantly stronger NMDAR mediated component.

Role of sensory pathway dlc interneuron

Our evidence suggests that dlc interneurons produce two types of excitation of contralateral neurons. Some neurons, particularly motoneurons, have a clear AMPAR component to their excitation. In response to skin stimulation this component can summate to produce firing from the resting state (Figs 7B, 8A). Other neurons receive weaker, mainly NMDAR mediated, excitation that is very unlikely to lead to firing from rest in normal saline with Mg^{2+} (Fig. 6). What is the function of these different types of excitation of contralateral neurons?

The faster AMPAR mediated excitation could produce the first, short latency, contralateral motor response seen when swimming starts in response to skin stimulation (Fig. 1A). A typical pattern of sensory pathway interneuron and motoneuron activity underlying this type of reflex action is shown in figure 9A. Similar short latency (< 15 msec) action potentials in response to skin stimulation were found in 28% of recordings from contralateral motoneurons (7/25; Fig. 8A) and 12% of those from contralateral interneurons (5/41).

A second role for AMPAR excitation in neurons excited by dlc interneurons is to produce “extra” contralateral motoneuron impulses at short latency when skin stimulation occurs during ongoing swimming (Sillar and Roberts, 1988b). These “extra” action potentials could lead to turning responses. Such responses had only previously been studied in 0 Mg^{2+} saline. We therefore re-examined the effects of tail skin stimulation on contralateral neurons at different phases of the fictive swimming cycle in saline with 1mM Mg^{2+}. Just as in 0 Mg^{2+} saline, we found that stimulation could evoke extra action potentials, recruit silent neurons (n = 11: 6 cINs, 3 aINs and 2 motoneurons), and produce a transient increase in swimming frequency (Fig. 9B).

DISCUSSION

Our first aim was to determine the organisation of a vertebrate spinal reflex: defining the neurons in the pathway that allows stimulation of the skin on one side of the body to excite motoneurons on the opposite side and produce a short-latency, crossed flexion response. By defining this synaptic pathway, we were then able to ask whether the properties of the synapses are uniform at this early stage in development, or whether they are tuned to their particular functions in the reflex pathway.

Definition of a primitive disynaptic reflex withdrawal pathway

We have used whole-cell patch recordings in the *Xenopus* tadpole spinal cord to seek synaptic connections between pairs of neurons that were identified using previously defined physiological and anatomical criteria (reviewed: Roberts et al., 2000; Li et al., 2001; Li et al., 2002). Evidence from 28 pairs shows that the primary skin sensory Rohon-Beard neurons that respond naturally to stroking the skin, directly excite sensory pathway dlc interneurons. These interneurons have somata and dendrites located dorsolaterally in the tadpole equivalent of the spinal dorsal horn. Their axons run ventrally across the spinal cord to form a decussating projection towards the brain corresponding to the spino-thalamic tract in adult vertebrates (Brodal and Brodal, 1981). The strength of the excitatory synapses from RB neurons to dlc interneurons, and the large sample size in the present recordings, gives us confidence that dlc interneurons form the pathway to carry excitation from skin touch to the other side of the spinal cord (Clarke and Roberts, 1984; Roberts and Sillar, 1990).

The output connections of sensory pathway dlc interneurons were shown using paired recordings with neurons on the opposite side that were active during fictive swimming. In 29 cases, dlc interneurons produced direct excitation of these neurons and in 6 of these cases the postsynaptic neuron was a motoneuron. This means that we have defined a minimal disynaptic pathway from cutaneous receptors on one side of the body to motoneurons on the other (Fig 1B). Such a pathway can explain short-latency contralateral responses to electrical skin stimulation (Fig 1A) and the normal contralateral flexion response seen in the whole behaving tadpole when the skin on one side of the trunk is stroked (Boothby and Roberts, 1995). This response is a primitive withdrawal reflex; it bends the trunk away from a stimulus and normally leads to the tadpole swimming away. Our evidence from paired recordings confirms earlier proposals on the mechanism of this reflex (Sillar and Roberts, 1992).

We know of no other case in the vertebrates where the neurons responsible for such a simple reflex have been defined. In mammals, withdrawal reflexes following skin stimulation are usually considered to be tri-synaptic with two layers of interposed interneurons. However, in two cases, central delay times of 1.5ms or less have been calculated (Illert et al., 1976; Fleshman et al., 1988). Similar short delays of 1.6ms were found in jaw opener responses to stimulation of the inferior dental nerve (Kidokoro et al., 1968). In all these cases the authors concluded that motoneurons must be excited via a disynaptic pathway following sensory nerve stimulation. The interneurons responsible have not of course been identified. It is important to remember that in the tadpole all connections are made by fine, unmyelinated axons (< 0.5 μm in diameter). The resulting slow central delay times explain why the reflex latency may appear relatively long for a simple disynaptic pathway.

As well as contralateral motoneurons, sensory pathway dlc interneurons also excite all classes of interneurons that are components of the central pattern generator for swimming (see Fig 1B). Descending interneurons (dINs) are thought to provide the glutamatergic excitatory drive to ipsilateral motoneurons during swimming (Dale and Roberts, 1985). If they are excited to fire by contralateral skin stimulation, they would form a trisynaptic path for a withdrawal reflex that could sum with more direct input to motoneurons. If glycinergic cINs are excited to fire, they would inhibit the stimulated side to prevent conflicting action. Excitation of spinal interneurons may also play a key role in the subsequent initiation of swimming.

Tuning of synaptic properties to function

Studying the reflex pathway has allowed us to see that the synapses made by primary sensory RB neurons are very different to those made by sensory pathway dlc interneurons. When recording in 0 Mg^{2+} saline the EPSPs from individual RBs to dlc interneurons were significantly larger and faster than those from individual dlc interneurons to contralateral neurons. Voltage clamp measurements on responses to skin stimulation show that an important difference is in the size of the fast, AMPAR mediated component of "conventional", dual-component glutamatergic synapses. The ratio of AMPAR/NMDAR currents was 28 for RB and only 1.5 for dlc interneuron synapses. The AMPAR mediated component dominates powerfully at RB synapses at early developmental stages. We have not measured spontaneous synaptic excitation but EPSPs and EPSCs have been recorded in TTX in presumed dlc interneurons, and were found to be large (Sillar and Roberts, 1988a; Rohrbough and Spitzer, 1999). A simple interpretation is that RB neurons may release ample transmitter at their synapses onto dlc interneurons where the post-synaptic density of AMPAR is high. In contrast to this, synapses from dlc interneurons to contralateral neurons are weak and produce small EPSPs and EPSCs. There is only evidence for significant AMPAR mediated excitation in some neurons. If the

recordings had been made in 1 mM Mg^{2+} saline, the remaining synapses would have appeared "silent" as they are mediated primarily by NMDARs.

What is the functional significance of these differences? The most obvious significance is that activity in individual sensory interneurons can be recruited by a few RB neurons while activity in contralateral neurons will require the convergence of input from many sensory interneurons. Behaviourally, it is possible to initiate contralateral responses with a stimulus that will excite very few sensory RB neurons (1 to 5), by stroking a tadpole on the trunk or tail with the tip of a fine hair (Boothby and Roberts, 1995). We can now see why. The strong synapses from RB neurons allow recruitment of many sensory interneurons, which in turn can provide sufficient convergence of excitation to produce activity in contralateral motoneurons. The differences in these synapses could reflect different stages in the same developmental programme for glutamatergic synapses. However, whether or not this is the case, it appears that the synapses are tuned to their function, as they must be in a behaving animal. The strong synapses onto sensory interneurons ensure that a response can occur to a relatively localised (small?) stimulus. The weaker synapses onto contralateral neurons may avoid over-excitation, but will also ensure that the contralateral flexion response has a higher safety margin. Reflex responses will therefore only occur following the concerted action of many sensory interneurons that follows a significant sensory stimulus.

Our evidence suggests that the fast AMPAR component of the excitation from dlc interneurons can sum in motoneurons to produce short latency reflex firing at rest and during swimming (Fig 9). What is the significance of the NMDA component of dlc interneurons excitation of contralateral neurons? It is possible that the slower, weaker, voltage-dependent NMDAR mediated excitation that would normally be blocked at rest, could be "gated-in" by the excitatory synaptic drive descending from the brainstem when swimming starts. In this way this excitation could contribute to a snowballing, positive feedback to help initiate motor activity. It could also be "gated-in" by the excitatory synaptic drive present during swimming (cf Reichert and Rowell, 1985). In this way, NMDAR mediated dlc interneuron excitation could have an influence beyond the simple reflex response, producing longer lasting increases in swimming frequency either directly, or indirectly by recruitment of premotor excitatory interneurons (Sillar and Roberts, 1988b, 1992).

Conclusion

We have defined the neuronal pathway for a simple withdrawal reflex in the frog tadpole. The evidence at this early stage in development shows that synapses at different steps in this pathway have very different properties that appear to be tuned to their functions in the reflex response. It is possible that these differences result from the sensory neurons and interneurons being at different stages in a common developmental program where synapses move from NMDA to AMPA mediated excitation. However, the only study on the development of these sensory neuron synapses in *Xenopus* has suggested the opposite, a move from more AMPA to more NMDA receptors (Rohrbough and Spitzer, 1999). Unlike developing brain areas, these spinal circuits have to function to produce reflexes and swimming from an early stage. It is therefore possible that the properties of the synapses arise "hard wired" and independent of prior activity (Renger et al., 2001; Ziv and Garner, 2001) rather than following a path from NMDAR to AMPAR mediated excitation depending on activity.

It will be fascinating to find if the sensory pathway dlc interneurons that we have defined in tadpoles are homologues of dorsal commissural interneurons defined by expression factors in the spinal cord of the developing mouse (Bermingham et al., 2001; Gowan et al., 2001).

REFERENCES

Bermingham NA, Hassan BA, Wang VY, Fernandez M, Banfi S, Bellen HJ, Fritzsch B, Zoghbi HY (2001) Proprioceptor pathway development is dependent on Math1. Neuron 30:411-422.

Boothby KM, Roberts A (1995) Effects of site and strength of tactile stimulation on the swimming responses of Xenopus laevis embryos. J Zool 235:113-125.

Brodal P, Brodal A (1981) The olivocerebellar projection in the monkey. Experimental studies with the method of retrograde tracing of horseradish peroxidase. J Comp Neurol 201:375-393.

Clarke JD, Roberts A (1984) Interneurones in the Xenopus embryo spinal cord: sensory excitation and activity during swimming. J Physiol (Lond) 354:345-362.

Clarke JD, Hayes BP, Hunt SP, Roberts A (1984) Sensory physiology, anatomy and immunohistochemistry of Rohon-Beard neurones in embryos of *Xenopus laevis*. J Physiol (Lond) 348:511-525.

Dale N (1985) Reciprocal inhibitory interneurones in the *Xenopus* embryo spinal cord. J Physiol (Lond) 363:61-70.

Dale N, Roberts A (1985) Dual-component amino-acid-mediated synaptic potentials: excitatory drive for swimming in *Xenopus* embryos. J Physiol (Lond) 363:35-59.

Feldman DE, Knudsen EI (1998) Experience-dependent plasticity and the maturation of glutamatergic synapses. Neuron 20:1067-1071.

Fleshman JW, Rudomin P, Burke RE (1988) Supraspinal control of a short-latency cutaneous pathway to hindlimb motoneurons. Exp Brain Res 69:449-459.

Gowan K, Helms AW, Hunsaker TL, Collisson T, Ebert PJ, Odom R, Johnson JE (2001) Crossinhibitory activities of Ngn1 and Math1 allow specification of distinct dorsal interneurons. Neuron 31:219-232.

Illert M, Lundberg A, Tanaka R (1976) Integration in descending motor pathways controlling the forelimb in the cat. 2. Convergence on neurones mediating disynaptic cortico-motoneuronal excitation. Exp Brain Res 26:521-540.

Kidokoro Y, Kubota K, Shuto S, Sumino R (1968) Reflex organization of cat masticatory muscles. J Neurophysiol 31:695-708.

Li WC, Soffe SR, Roberts A (2002) Spinal inhibitory neurons that modulate cutaneous sensory pathways during locomotion in a simple vertebrate. J Neurosci 22:10924-10934.

Li WC, Perrins R, Soffe SR, Yoshida M, Walford A, Roberts A (2001) Defining classes of spinal interneuron and their axonal projections in hatchling *Xenopus laevis* tadpoles. J Comp Neurol 441:248-265.

Reichert H, Rowell CH (1985) Integration of nonphaselocked exteroceptive information in the control of rhythmic flight in the locust. J Neurophysiol 53:1201-1218.

Renger JJ, Egles C, Liu G (2001) A developmental switch in neurotransmitter flux enhances synaptic efficacy by affecting AMPA receptor activation. Neuron 29:469-484.

Roberts A, Sillar KT (1990) Characterization and Function of Spinal Excitatory Interneurons with Commissural Projections in *Xenopus laevis* embryos. Eur J Neurosci 2:1051-1062.

Roberts A, Hill NA, Hicks R (2000) Simple mechanisms organise orientation of escape swimming in embryos and hatchling tadpoles of *Xenopus laevis*. J Exp Biol 203:1869-1885.

Roberts A, Walford A, Soffe SR, Yoshida M (1999) Motoneurons of the axial swimming muscles in hatchling *Xenopus* tadpoles: features, distribution, and central synapses. J Comp Neurol 411:472-486.

Rohrbough J, Spitzer NC (1999) Ca^{2+}-permeable AMPA receptors and spontaneous presynaptic transmitter release at developing excitatory spinal synapses. J Neurosci 19:8528-8541.

Sillar KT, Roberts A (1988a) Unmyelinated cutaneous afferent neurons activate two types of excitatory amino acid receptor in the spinal cord of *Xenopus laevis* embryos. J Neurosci 8:1350-1360.
Sillar KT, Roberts A (1988b) A neuronal mechanism for sensory gating during locomotion in a vertebrate. Nature 331:262-265.
Sillar KT, Roberts A (1992) The role of premotor interneurons in phase-dependent modulation of a cutaneous reflex during swimming in *Xenopus laevis* embryos. J Neurosci 12:1647-1657.
Soffe SR (1993) Two distinct rhythmic motor patterns are driven by common premotor and motor neurons in a simple vertebrate spinal cord. J Neurosci 13:4456-4469.
Soffe SR (1997) The pattern of sensory discharge can determine the motor response in young *Xenopus* tadpoles. J Comp Physiol [A] 180:711-715.
Yoshida M, Roberts A, Soffe SR (1998) Axon projections of reciprocal inhibitory interneurons in the spinal cord of young *Xenopus* tadpoles and implications for the pattern of inhibition during swimming and struggling. J Comp Neurol 400:504-518.
Zhu JJ, Malinow R (2002) Acute versus chronic NMDA receptor blockade and synaptic AMPA receptor delivery. Nat Neurosci 5:513-514.
Ziv NE, Garner CC (2001) Principles of glutamatergic synapse formation: seeing the forest for the trees. Curr Opin Neurobiol 11:536-543.

Figure legends

Figure 1

The spinal flexion reflex. *A*, Recordings from left (*Lvr*) and right (*Rvr*) mid-trunk ventral roots to show short latency activity (*arrow*) in left side motoneurons following a 1 msec current pulse to the right tail skin (at artifact: *stim right*). Five traces overlapped. *B*, Spinal cord neurons that may be parts of the response pathway from skin touch on the right side to motoneuron activity on the left. The direct pathway leads from skin touch sensory RB neurons (*RB*) to sensory pathway dlc interneurons (*dlc*), across the ventral commissure to motoneurons (*mn*) on the left side. Other possible targets for dlc interneuron excitation are Central Pattern Generator (CPG) interneurons active during swimming. These are: ascending interneurons (*aIN*) that produce glycinergic inhibitory gating of dlc interneurons during swimming (Li *et al*., 2002), glycinergic reciprocal inhibitory commissural interneurons (*cIN*), and descending interneurons (*dIN*) that are thought to produce glutamatergic excitation during swimming. Open circles represent populations of interneurons; small open triangles are presumed glutamatergic synapses.

Figure 2

Paired recordings show that RB sensory neurons strongly excite sensory pathway dlc interneurons at a short and constant latency. *A*, (a) Tadpole 5 to 6 mm long and a scale diagram of the CNS to show filled RB and dlc interneuron. The dlc axon (*dotted*) is on the opposite left side; hindbrain to midbrain border indicated (*h/m*). (b) RB and dlc interneuron at the cut dorsal edge of the spinal cord in the 5th segment on the right side. The spherical RB soma has an ascending axon and descending axon (*arrowhead*) with possible contact sites onto dlc dendrites (*white arrows*). The multipolar dlc soma has oblique dendrites and a ventral initial process leading to a ventral commissural axon (*black arrow*). (c) Current injection evoking an action potential in RB leads to a large EPSP in the dlc interneuron at short latency (three traces overlapped; the whole EPSP, trace length = 100 msec, is shown in d). The RB impulse causes a small artifact in the dlc interneuron (*arrowhead*). *B*, (a) In this case the RB is caudal to the dlc interneuron. (b) Ascending RB axon (*arrowhead*) with possible contacts to the dlc interneuron (*white arrows*), that has a commissural axon (*black arrow*). (c) Current evoked RB action potentials lead to variable amplitude dlc interneuron EPSPs, 2 of which reach threshold for a dlc action potential. *C*, (a) An example where current evoked action potentials in a RB in the 6th segment lead to large, reliable, constant latency EPSPs in a dlc interneuron. Even with –30 pA hyperpolarising current injected into the dlc interneuron, these EPSPs can reach threshold and evoke dlc interneuron action potentials. (b) The reliability of the EPSP is shown by repeated current pulses to the RB neuron.

Figure 3

Effects of glutamate receptor antagonists on EPSPs evoked in a dlc interneuron by RB action potentials. *A*, Scale drawings of the CNS from the right side to show (a) the location of the RB soma and its descending axon passing the dlc interneuron soma; (b) at higher magnification, a possible contact point (*arrow*) of the RB axon and a dendrite emerging from the dlc interneuron soma. The ventral, commissural dlc interneuron axon branches on the opposite side of the cord. *B*, *Top two traces:* current evoked RB impulses (*RB*) produce large EPSPs in the dlc interneuron (*dlc*). *Bottom trace:* whole time course of dlc interneuron EPSPs. *C*, The EPSP is blocked by bath application of NBQX; partially recovers in control; and is little affected by D-AP5. After recovery in control, the EPSP is

blocked by simultaneous application of 2.5 μM NBQX and 25 μM D-AP5 and recovers in control. Antagonists were drop-applied; 3 overlapped traces in each.

Figure 4

Effects of glutamate receptor antagonists on excitation in dlc interneurons produced by electrical stimulation of RB neurites in the skin. *A*, CNS from the right side to show (a) the location of the dlc soma and contralateral axon (*dotted*), and (b) the characteristic dlc soma with emerging dendrites (*arrow*) and ventral axon (*arrowhead*). *B*, Current-clamp recordings where in control the RB stimulus (*arrow*) produces an EPSP and action potential. The EPSP is strongly reduced in NBQX, little affected by D-AP5 and blocked by combined application. *C*, Another dlc interneuron, voltage-clamped at –65 mV, shows a large, fast inward current in response to the RB stimulus (*arrow*). The large, fast component is blocked by 2.5 μM NBQX to leave a small, slow component that is blocked by 25 μM D-AP5. Antagonists were drop-applied; 3 overlapped traces in each case. 2 μM strychnine was in the saline to block glycinergic inhibition on the dlc interneuron.

Figure 5

Paired recordings show that sensory pathway dlc interneurons excite a contralateral motoneuron and commissural IN at short and constant latency. *A*, (a) Scale drawing of the CNS viewed from the left side to show the dlc interneuron with multipolar soma at the dorsal edge of the spinal cord on the right side has a ventral commissural axon that branches after crossing to the left side. Here, its ascending axon has possible contact sites onto a motoneuron. (b) Multipolar motoneuron soma at 4th segment on left side with a possible contact point from the dlc axon (*arrowhead*) on its dendrites (*arrow*). The mn has a ventral descending axon and a broken peripheral axon (*). *B*, Current injection evoking an action potential in the dlc interneuron shown in (A), leads to a small EPSP in the mn at constant and short latency. Overlapped traces. *C*, The same record as (B) to show the long duration of the EPSP. *D*, (a) Scale drawing to show a right dlc interneuron and left cIN. (b) Possible synaptic contact (*arrow*) between the dlc axon (*arrowhead*) and cIN dendrite. *E*, *F*, Small, slow rise cIN EPSPs produced by dlc spikes evoked by current injection. The artifact (*arrowhead*) caused by the presynaptic dlc action potential has not been subtracted.

Figure 6

Paired recordings show that sensory pathway dlc interneurons excite contralateral neurons by activating glutamate receptors. *A*, (a) Scale drawings of the CNS viewed from the left side to show a dlc interneuron on the right side of the spinal cord with a commissural axon that branches on the left side where its ascending axon (*dotted*) has possible contact sites onto an aIN. (b) The multipolar dlc interneuron soma has an ascending axon (*arrowhead*) with possible contact points (*arrow*) on dendrites of the aIN, whose axon (*) has been omitted for clarity. *B*, (a) Current injection evoking an action potential in the dlc interneuron shown in (A) leads to slow rise, small EPSPs in the aIN at short latency (4 overlapped traces). (b) The same neuron pair to show the long duration EPSP is blocked by 50 μM D-AP5 but is little affected by 5 μM NBQX. *C*, Small, short latency EPSPs (6 overlapped traces) in a motoneuron (*mn*) produced by current evoked dlc interneuron impulses (*dlc*). *D*, The same record as (C) showing the long duration of the EPSP. *E*, Effects of glutamate receptor antagonists on EPSPs evoked in the motoneuron by dlc interneuron action potentials. The long, slow component of the EPSP is blocked by 50 μM D-AP5 and recovers in wash. The fast initial component is blocked by 5 μM NBQX. After recovery in

wash the EPSP is blocked by simultaneous application of 5 μM NBQX and 50 μM D-AP5 and returns after wash. Antagonists were drop-applied; 3 overlapped traces.

Figure 7

Pharmacology of responses to contralateral skin stimulation in a descending interneuron (dIN). *A*, (a) Scale drawing of the CNS viewed from left side to show the dIN on the left side of the spinal cord with a descending axon. (b) Details of the dIN multipolar soma with short dendrites (*arrow*) and a descending axon (*arrowhead*). *B*, Contralateral tail skin stimulation (*arrow*) produces a slow rise EPSP at constant latency that in one trace evokes a spike in the dIN. *C*, Pharmacology of EPSCs in the same dIN at a holding potential of –65 mV. D-AP5 blocks a slow component to reveal a small fast EPSC (*) which is blocked by NBQX. Antagonists were microperfused and the circulating saline contained 10 μM mecamylamine and 2 μM strychnine to block any cholinergic and glycinergic currents; 3 overlapped traces.

Figure 8

Pharmacology of excitation evoked by contralateral skin stimulation (*at arrows*) and effects of Mg^{2+}. For each example, the inital (*left*) and whole (*right*) response is shown. *A*, EPSPs in a motoneuron which evoke an action potential at higher stimulus levels. Overlapped traces. *B*, In the same mn, averaged EPSCs in control saline, NBQX and D-AP5 as used in measurements of AMPAR/NMDAR current ratios. *C*, Similar averaged EPSCs from a cIN. *E*, Effect of 1 mM Mg^{2+} on averaged slow rise EPSCs in another mn. Antagonists and Mg^{2+} were microperfused close to the recorded neuron and the circulating saline contained 10 μM mecamylamine and 2 μM strychnine.

Figure 9

Roles of excitation from dlc interneurons. *A*, Excitation of a contralateral mn from rest. Paired recording from a right side sensory pathway dlc interneuron (*dlc*) and a left side motoneuron (*mn*); the same recording as Figure 5A. Responses to increasing the strength of a current pulse to stimulate the right tail skin (*arrow*). At higher stimulus levels both dlc and mn fire an action potential at latencies of ~5 and ~10 msec. *B*, Excitation during swimming. When the right tail skin is stimulated (*arrow*) swimming frequency increases in the right side ventral root record at the 10^{th} segment (*right vr*), and CPG neurons on the left side (*left aIN* and *left mn*) are recruited to fire action potentials. The mn even fires 3 action potentials (*).

Figure 1

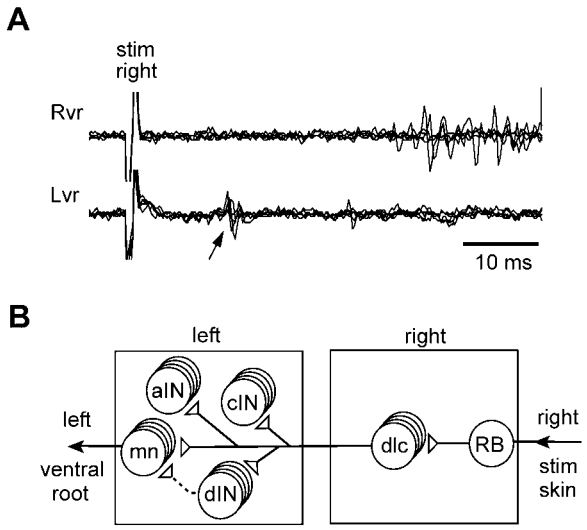
A
stim
right
Rvr
Lvr
10 ms
B
left
right
aIN
cIN
left
mn
dlc
RB
right
ventral
root
dIN
stim
skin

Figure 2

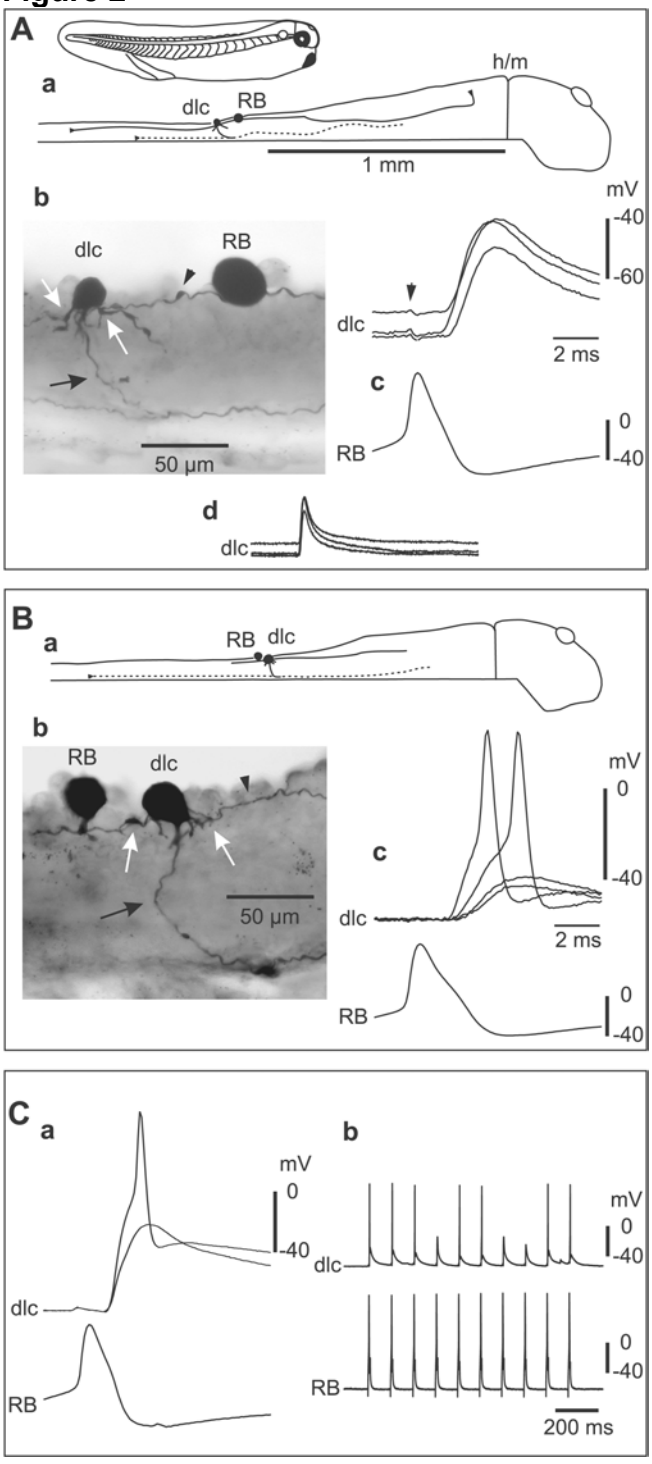
A
a
h/m
dlc
RB
1 mm
b
dlc
RB
50 µm
mV
-40
-60
dlc
2 ms
c
RB
0
-40
d
dlc
B
a
RB
dlc
b
RB
dlc
50 µm
c
mV
0
-40
dlc
2 ms
RB
0
-40
C
a
mV
0
-40
dlc
RB
b
mV
0
-40
dlc
0
-40
RB
200 ms

Figure 3

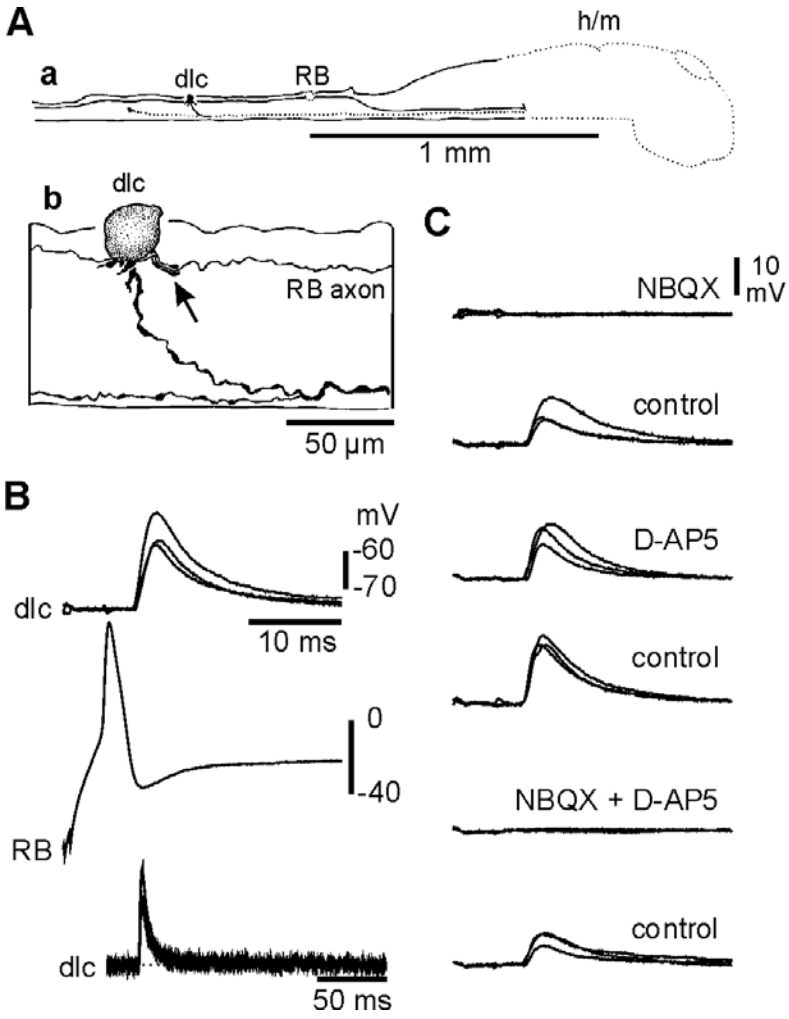
A
a
dlc
RB
h/m
1 mm
b
dlc
RB axon
50 µm
B
mV
-60
-70
dlc
10 ms
0
-40
RB
dlc
50 ms
C
NBQX
10 mV
control
D-AP5
control
NBQX + D-AP5
control

Figure 4

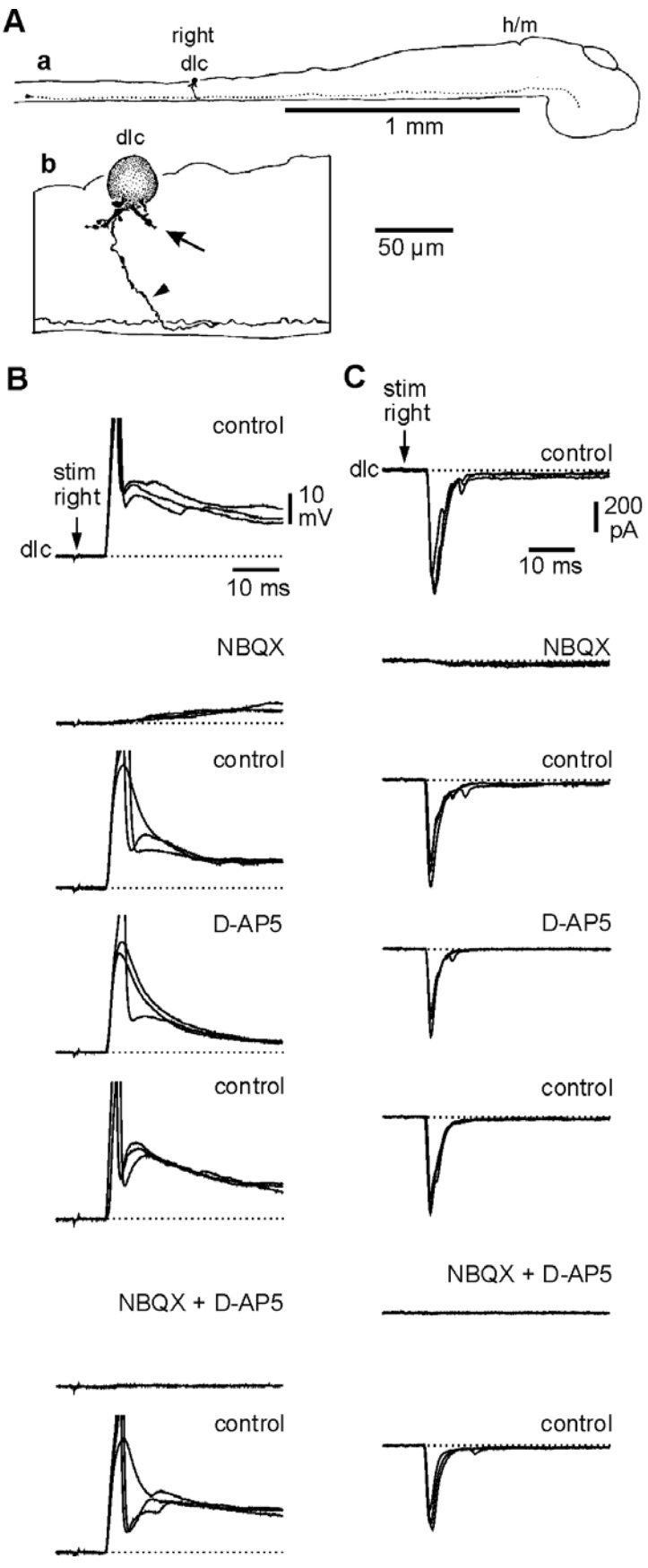
A
a
right
dlc
h/m
1 mm
dlc
b
50 µm
B
control
stim
right
10
mV
dlc
10 ms
NBQX
control
D-AP5
control
NBQX + D-AP5
control
C
stim
right
dlc
control
200
pA
10 ms
NBQX
control
D-AP5
control
NBQX + D-AP5
control

Figure 5

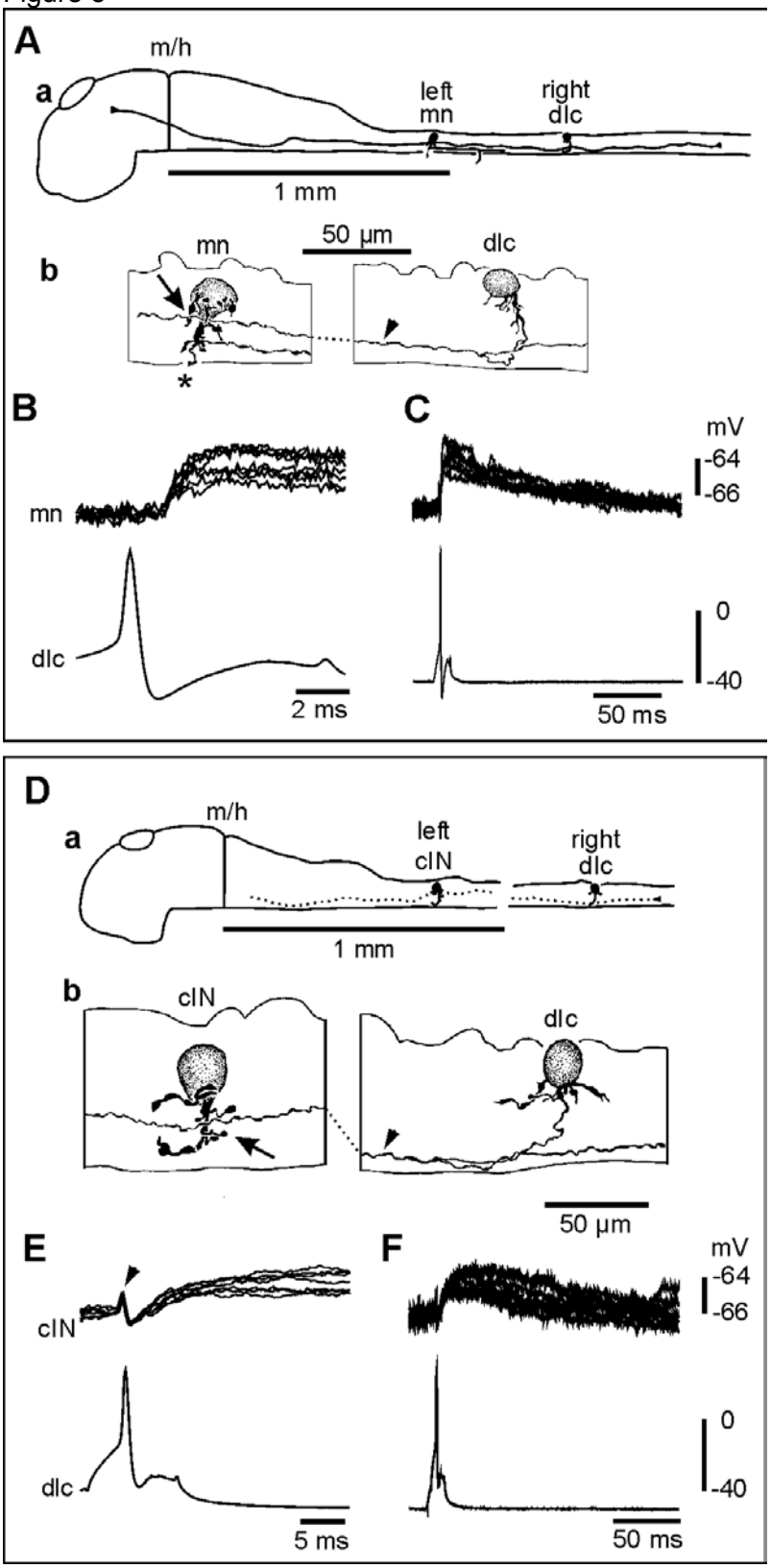
A
m/h
a
left
mn
right
dlc
1 mm
b
mn
50 µm
dlc
*
B
C
mn
mV
-64
-66
dlc
0
-40
2 ms
50 ms
D
m/h
a
left
cIN
right
dlc
1 mm
b
cIN
dlc
50 µm
E
F
cIN
mV
-64
-66
dlc
0
-40
5 ms
50 ms

Figure 6

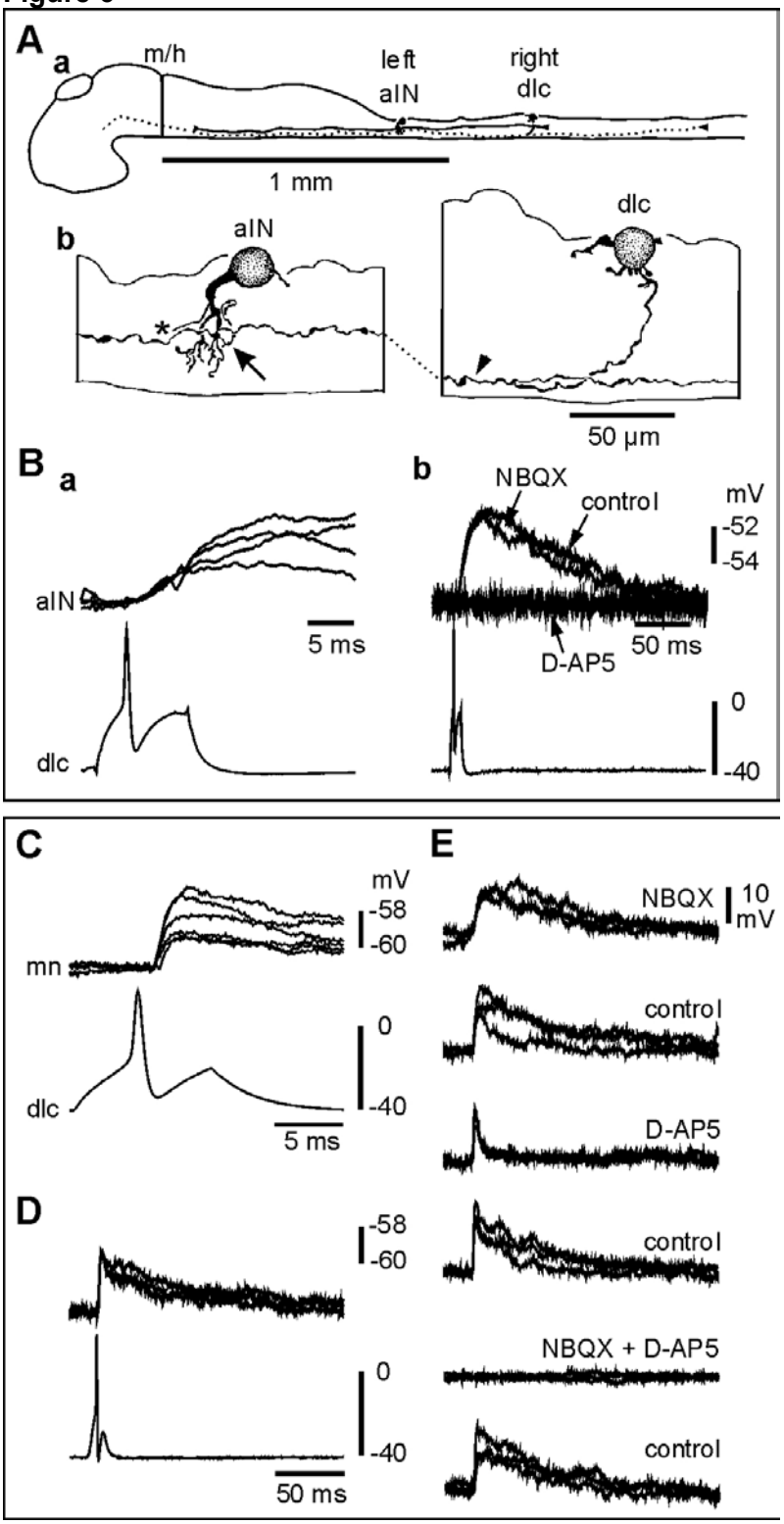
A
a
m/h
left
aIN
right
dlc
1 mm
b
aIN
dlc
50 µm
B
a
aIN
5 ms
dlc
b
NBQX
control
mV
-52
-54
50 ms
D-AP5
0
-40
C
mV
-58
-60
mn
0
-40
dlc
5 ms
D
-58
-60
0
-40
50 ms
E
NBQX
10
mV
control
D-AP5
control
NBQX + D-AP5
control

Figure 7

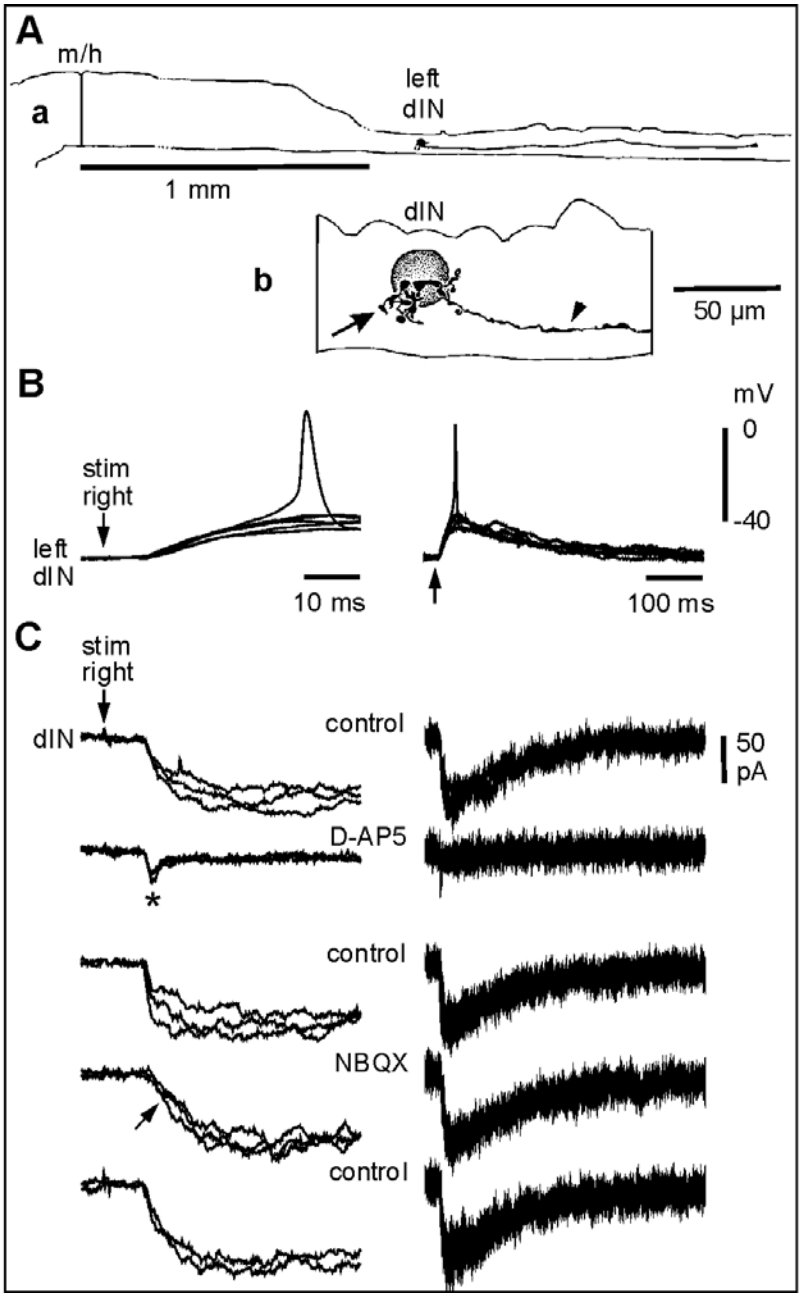
A
m/h
a
left
dIN
1 mm
dIN
b
50 µm
B
mV
0
-40
stim
right
left
dIN
10 ms
100 ms
C
stim
right
dIN
control
50
pA
D-AP5
*
control
NBQX
control

Figure 8

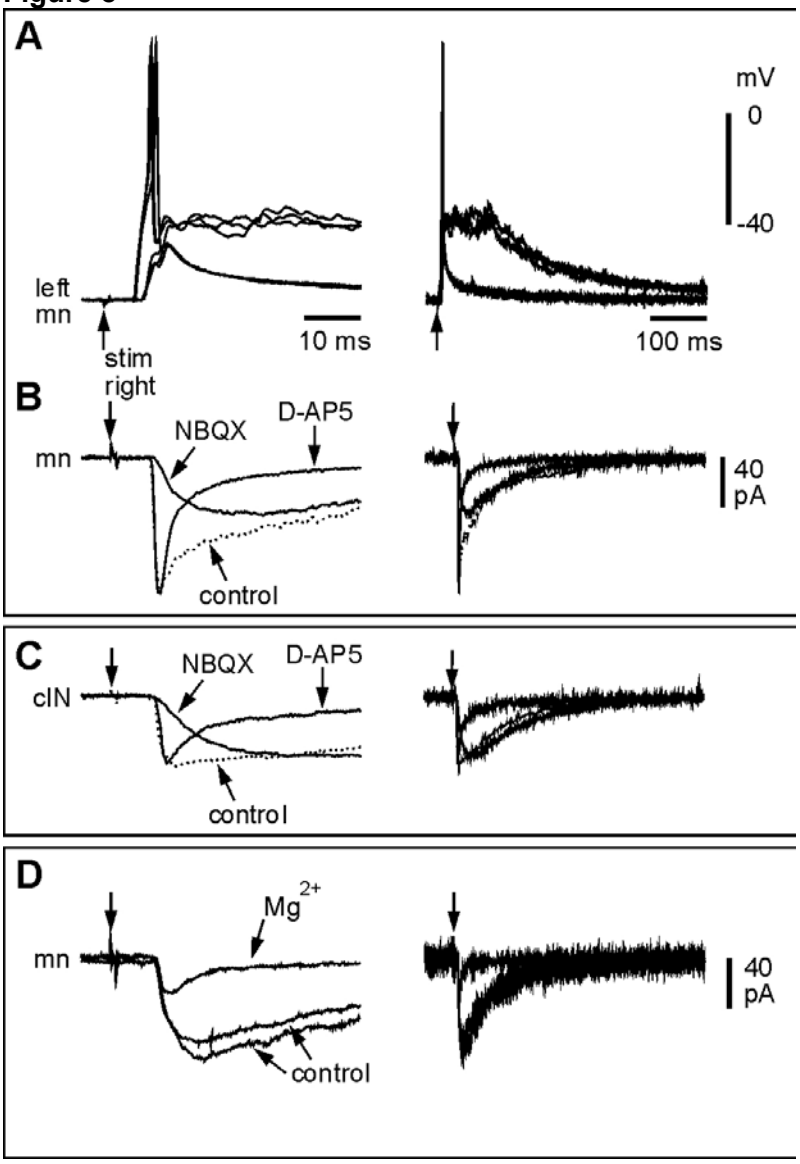
A
mV
0
-40
left
mn
stim
right
10 ms
100 ms
B
mn
NBQX
D-AP5
control
40
pA
C
cIN
NBQX
D-AP5
control
D
mn
Mg2+
control
40
pA

Figure 9

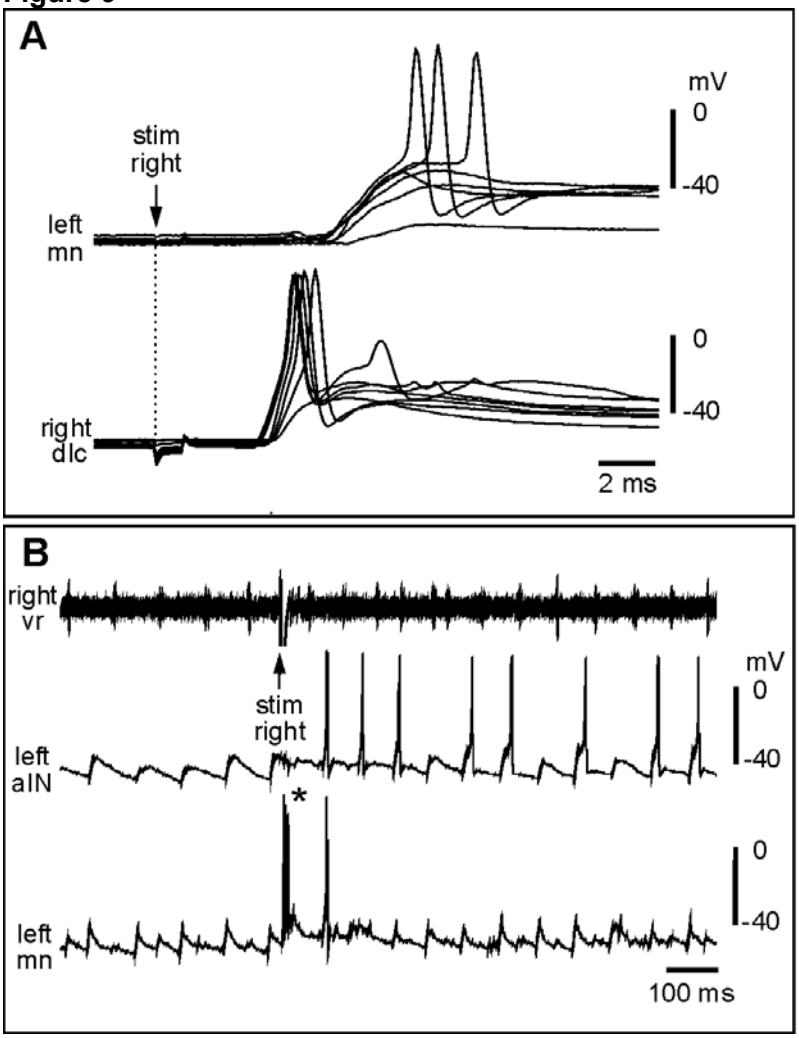
A
mV
0
-40
stim
right
left
mn
0
-40
right
dlc
2 ms
B
right
vr
stim
right
mV
0
-40
left
aIN
*
0
-40
left
mn
100 ms